Progress In Electromagnetics Research M, Vol. 82, 95–105, 2019

Metamaterial Inspired Structure with Offset-Fed Microstrip Line for Multi Band Operations

Balasubramanian Murugeshwari[1, *], Raphael Samson Daniel[1], and Singaravelu Raghavan[2]

Abstract—A miniaturized rectangle-shaped complementary split ring radiating element with an offset-fed microstrip line is reported for multiband operations. The fabricated antenna with a compact size of $19 \times 19 \times 1.6\,\text{mm}^3$ is designed on an FR-4 substrate with loss tangent $\tan\delta = 0.02$ and dielectric constant (ε_r) of 4.4. Multiband and antenna miniaturization are achieved by a complementary split ring radiating element, and it produces an impedance bandwidth of 40 MHz resonance at 3.03 GHz, 40 MHz resonance at 3.66 GHz, and 1470 MHz resonance at 5.5 GHz. The passband behaviour of the complementary split ring radiating element is studied in detail for obtaining multiband abilities of the miniaturized antenna. The metamaterial property of the complementary split ring radiating element is analyzed, by which the negative permittivity (ε) existence and the new resonance frequency are confirmed. The fabricated antenna shows optimum performance at the measured radiation characteristics.

1. INTRODUCTION

Metamaterial inspired antennas have been synthesized for multiband antenna design due to the verified extraordinary EM wave properties [1]. Metamaterial is a man-made homogenous structure composite to exhibit negative permeability (μ) and negative permittivity (ε) for performance enhancement of antenna [2]. Split Ring Resonator (SRR) exhibits negative value of permeability, and Complementary Split Ring Resonator (CSRR) exhibits negative value of permittivity. Single Negative Metamaterial (SNG) is governed by either μ-negative material or ε-negative material, and Double Negative Metamaterial (DNG) is governed by both μ-negative material and ε-negative material [3]. Negative permittivity material is used to design new microwave components such as filters [4], power divider [5], branch line coupler [6], and multiband antenna design [7]. Due to the sub-wavelength resonator CSRR employs an antenna miniaturization [8] and bandwidth improvement [9]. The ε-negative metamaterial has spurred in millimeter wave frequency, such as phase shifter [10], circular polarization [11], and eliminates cross polarization [12]. Metamaterial absorber can be used for energy harvesting [13], multi-band polarization [14], and wide-band characteristics [15].

The objective of this paper is to investigate the performance of CSRR based radiating element with an offset-fed microstrip line for achieving multiband operation and 64% of antenna miniaturization. CSRRs passband behaviour and negative permittivity (ε) characteristics are discussed in detail for good understanding. The antenna is designed to operate in WiMAX (3.03/3.66 GHz) and WLAN (5.5 GHz) applications.

Received 11 March 2019, Accepted 9 June 2019, Scheduled 25 June 2019

* Corresponding author: Balasubramanian Murugeshwari (bmwinece@gmail.com).

[1] Department of Electronics and Communication Engineering, K. Ramakrishnan College of Engineering, Samayapuram, India. [2] National Institute of Technology, Trichirappalli 620015, India.

2. PROPOSED ANTENNA AND SIMULATED RESULTS

The evolution steps of the proposed antenna design are shown in Fig. 1. The designed antenna is developed from a single resonance conventional monopole antenna as shown in evolution step (A) of Fig. 1. This conventional monopole antenna contributes a single resonance frequency of 5 GHz. In order to achieve a multiband and antenna miniaturization from this single band, the radiating element is reformed to arrange two pairs of complementary split rings as shown in evolution step (B) of Fig. 1.

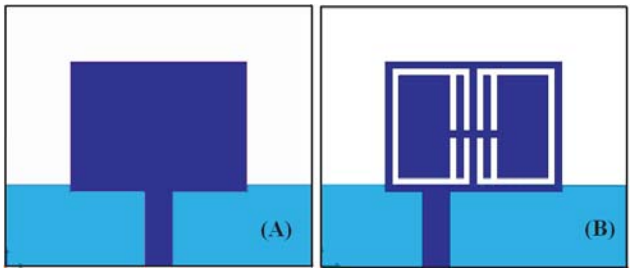

Figure 1. Evolution steps of antenna design.

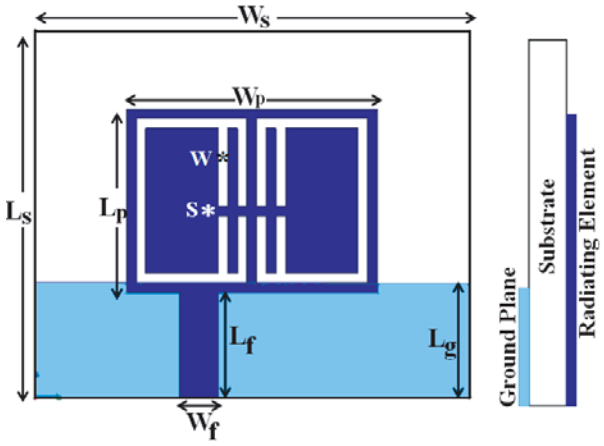

Figure 2. Antenna geometry and its side view.

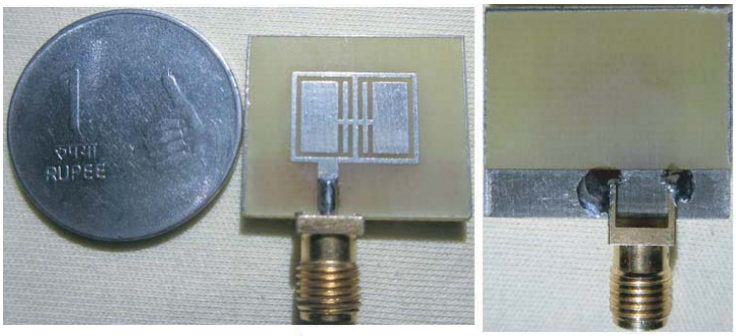

(a) (b)

Figure 3. Fabricated antenna. (a) Top view. (b) Bottom view.

Table 1. Dimensions of the proposed antenna.

Parameter	Dimension (mm)
L_s	19
W_s	19
L_P	13.04
W_P	9.58
L_f	5.51
W_f	2
L_g	6
S	0.5
W	0.5

The complementary split ring is capable of generating multiband resonance characteristics according to structural alignment of the metamaterial radiating element. The slot width (W) and the metal portion between the slots (S) are described constant for homogeneity. Now, the designed antenna offers two lower resonance frequencies for realizing 64% of compactness. The perspective view of the designed antenna is depicted in Fig. 2, and its dimensions are detailed in Table 1. The fabricated antenna is exposed in Fig. 3.

Ansoft HFSS V.15 electromagnetic software is utilized to simulate the reflection coefficient S_{11} (dB) of the proposed antenna. The simulated reflection coefficient S_{11} (dB) of the conventional monopole antenna (A) and prototype antenna (B) is shown in Fig. 4. It is perceived that the designed antenna exposes triple resonance frequencies of 3.03 GHz, 3.66 GHz, and 6 GHz. These resonance characteristics are confirmed by analyzing the complementary split ring under three cases: (i) closed complementary

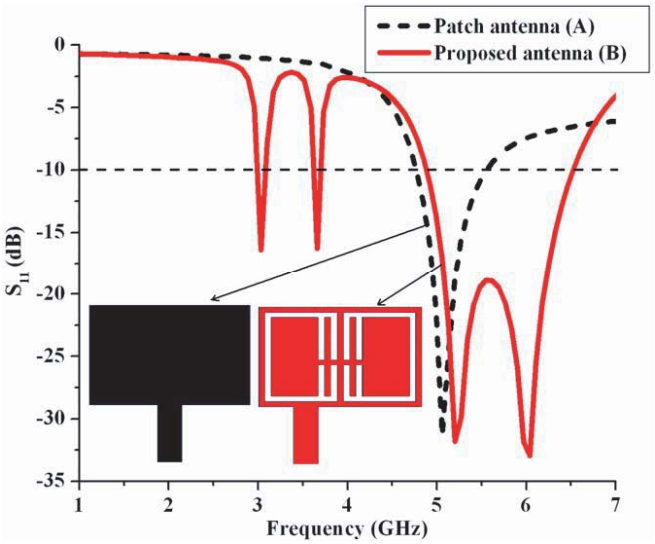

Figure 4. Reflection coefficient S_{11} (dB) of the antenna evolution steps.

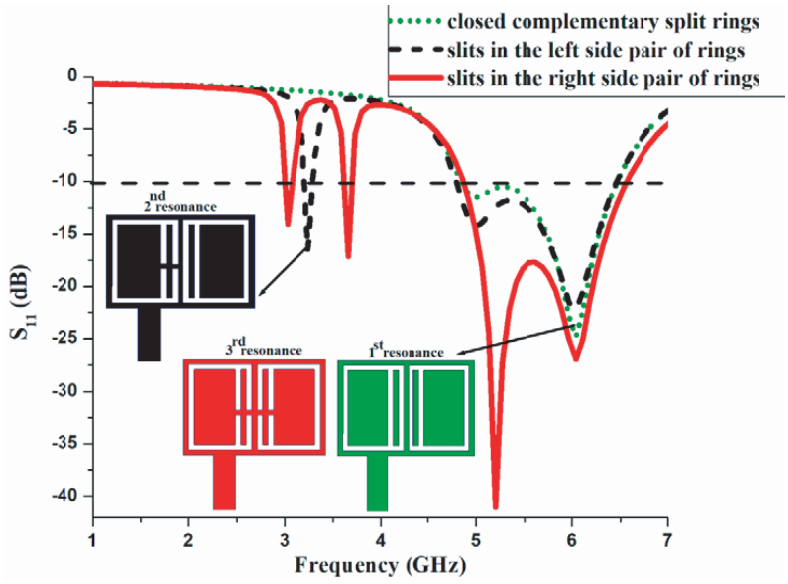

Figure 5. Reflection coefficient S_{11} (dB) of the three cases (i) closed complementary split rings, (ii) case i, along with slits in the left side pair of rings, (iii) case ii, along with slits in the right side pair of rings (proposed antenna).

split rings, (ii) case i, along with slits in the left side pair of rings, (iii) case ii, along with slits in the right side pair of rings (proposed antenna). Fig. 5 illustrates the simulated reflection coefficient S_{11} (dB) of the three cases with a conforming inset figure, which defines their geometries. It is examined that new resonance frequencies occur at 6 GHz (1st resonance), 3.03 GHz (2nd resonance), and 3.66 GHz (3rd resonance) due to cases (i), (ii), and (iii) structural alignment, respectively. The prototype antenna covers an impedance bandwidth of 80 MHz (3–3.08 GHz) centered at 3.03 GHz, 50 MHz (3.63–3.68 GHz) centered at 3.66 GHz, and 1640 MHz (4.88–6.52 GHz) centered at 5.5 GHz.

The simulated current distribution of the proposed antenna is depicted in Fig. 6. It describes that at lower resonance frequencies 3.03 GHz and 3.66 GHz, the current is concentrated around the left side complementary split ring, and at a higher resonance frequency, the current is concentrated around the slit and feed line of the monopole antenna.

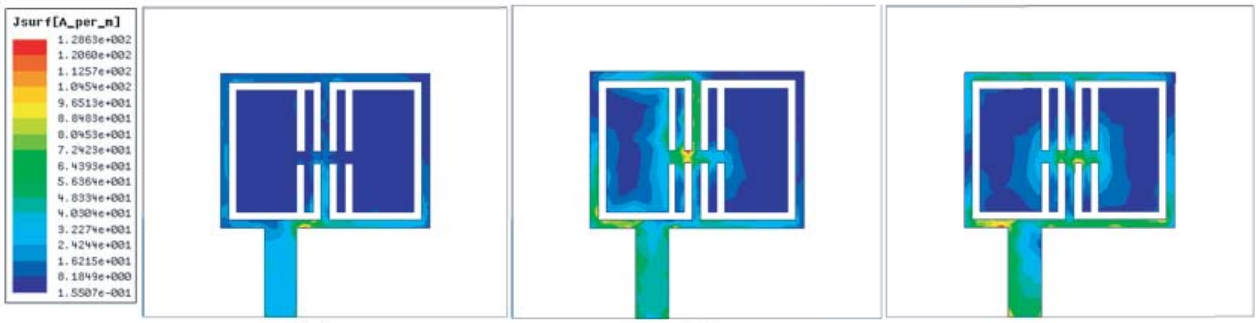

(a) (b) (c)

Figure 6. Simulated current distribution of the proposed antenna at (a) 3.03 GHz, (b) 3.66 GHz and (c) 5.5 GHz.

3. PARAMETRIC STUDY

The position of the microstrip feed (d) creates a significant role in governing the multiband and bandwidth improvement. It offers better impedance matching 50 Ω for operating frequencies. This

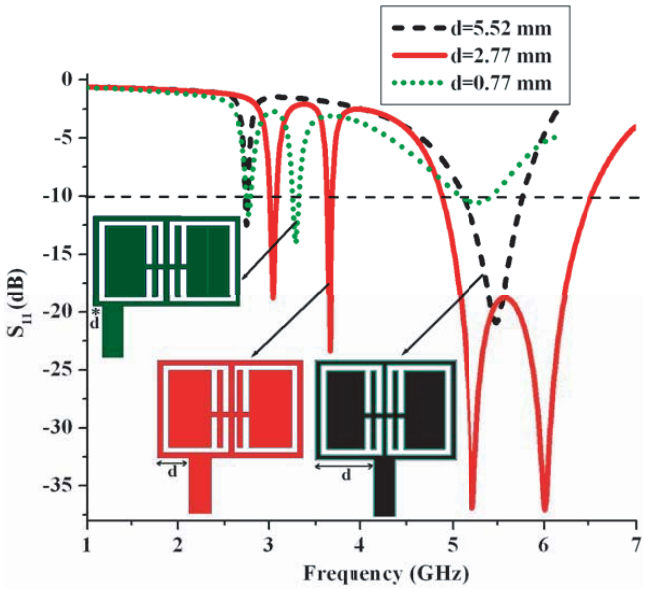

Figure 7. Reflection coefficient S_{11} (dB) of the antenna for various distances of the microstrip feed position.

is confirmed by performing a parametric analysis. Fig. 7 illustrates the parametric analysis on the microstrip feed position 'd' from the center. It is examined that center feed position yields dual-band characteristics, and offset microstrip line offers multiband at the distance of $d = 2.77$ mm.

The equivalent circuit of the proposed antenna is shown in Fig. 8. The slit gap 'S' produces inductance (L_0) effect, and a slot (W) produces the capacitance (C_c) effect. Thus, the reduction in inductance value offers a lower resonance frequency and improves the quality factor due to parallel combination of capacitance.

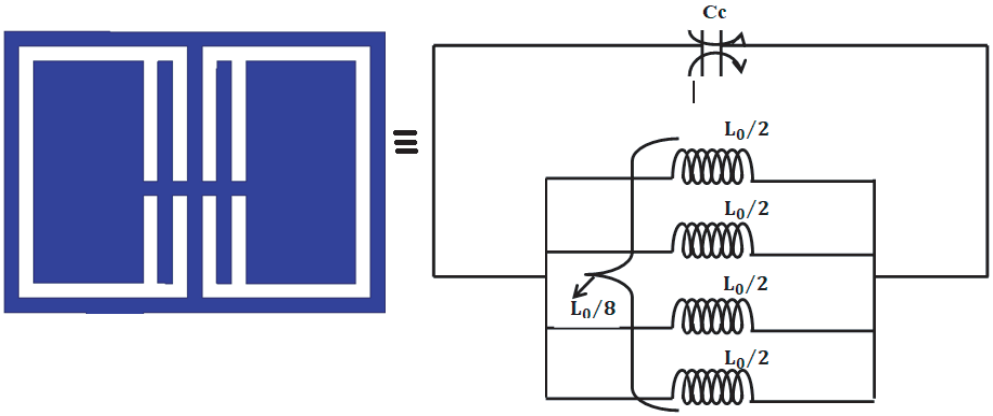

Figure 8. Equivalent circuit of the proposed antenna.

Similarly, the slit gap 'S' creates a significant role in governing the lower resonance frequency for achieving antenna miniaturization. Fig. 9 depicts the parametric analysis on the reflection coefficient of the proposed antenna for various slit gaps 'S' extending from 0.5 mm to 1.25 mm with incremental step of 0.25 mm. It is exposed that when the slit gap 'S' decreases, a narrow lower resonance frequency of 3.03 GHz is obtained. Hence, $S = 0.5$ mm is selected for fabrication to attain optimum performance of the antenna.

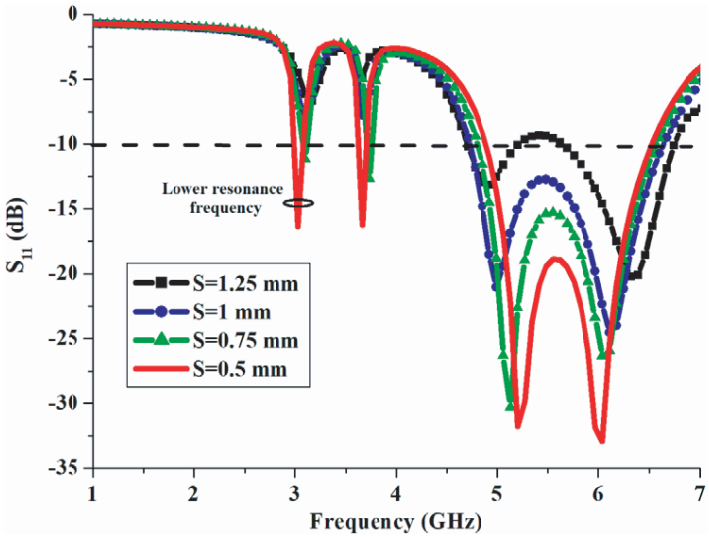

Figure 9. Reflection coefficient S_{11} (dB) of the antenna for various slit gap 'S'.

The slit effect on the complementary split ring radiating element is shown in Fig. 10. It represents that radiating element with a slit produces a narrow electric resonance for attaining antenna miniaturization and multiband characteristics due to the existence of pass band (S_{11}) in

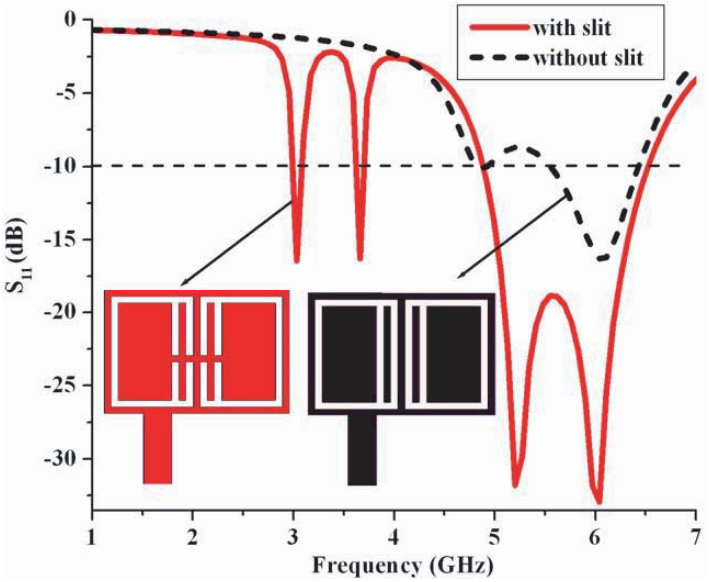

Figure 10. Slit effect on the complementary split ring radiating element.

the S-parameters. Radiating element without slit dose not create metamaterial property (negative permittivity) for attaining a new resonance frequency.

4. ANALYSIS OF COMPLEMENTARY SPLIT RING

The complementary split ring radiating element generates the passband (S_{11}) behaviour, which is examined by effective medium theory [16]. Here the radiating element is positioned inside a waveguide setup and is exposed to an EM wave along the input port of the waveguide. S-parameters S_{11} and S_{21} are measured through the output port of the waveguide. From these S-parameters, the values of permittivity (ε_r) and permeability (μ_r) are computed using Nicolson Ross Weir (NRW) equations [17].

$$\varepsilon_r = \frac{2}{jk_0d} * \frac{1 - V_1}{1 + V_1} \tag{1}$$

$$\mu_r = \frac{2}{jk_0d} * \frac{1 - V_2}{1 + V_2} \tag{2}$$

where

$$\begin{aligned} V_1 &= S_{21} - S_{11} \\ V_2 &= S_{21} + S_{11} \\ k_0 &= \text{Wave number of free space} \\ d &= \text{substrate thickness} \end{aligned}$$

The passband (S_{11}) characteristics of the rectangular radiating element and complementary split ring radiating element are depicted in Fig. 11. It shows that the complementary split ring radiating element offers new passbands correlated with the rectangular radiating element. These passbands are responsible for obtaining multiband characteristics of the proposed antenna. The extracted negative permittivity (ε) of the proposed antenna is shown in Fig. 12. It describes that the negative permittivity is confirmed due to passband behaviour. The negative permittivity is observed for frequencies around 3 GHz, 3.66 GHz, and 6 GHz, and this is where the antenna has exhibited new resonance frequencies in the input reflection coefficient S_{11} (dB) characteristics. Thus, it is proved that the complementary split ring radiating element governs for attaining antenna miniaturization and multiband.

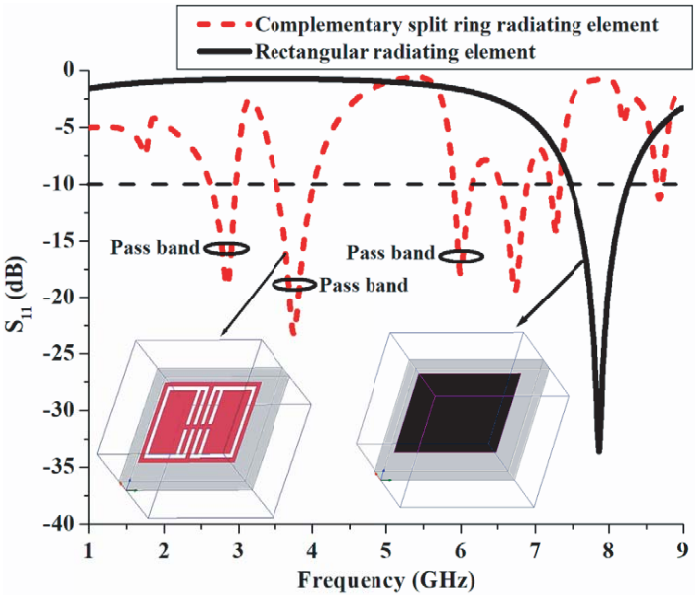

Figure 11. Passband (S_{11}) characteristics of the rectangular radiating element and complementary split ring radiating element.

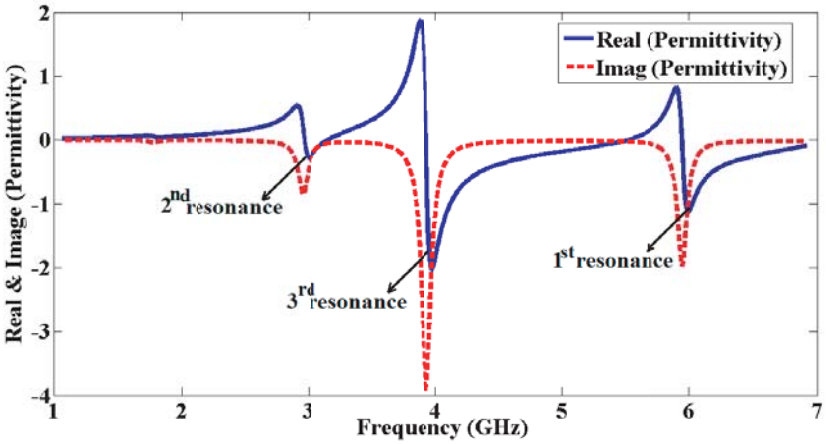

Figure 12. Real and imaginary parts of permittivity.

5. MEASUREMENT RESULTS

The simulated and measured reflection coefficients S_{11} (dB) of the antenna are shown in Fig. 13. Numerical values are displayed in Table 2. Experimental result matches simulated results perfectly. Measured S_{11} (dB) covers the impedance bandwidth of 40 MHz (2.98–3.02 GHz) centered at 3 GHz, 40 MHz (3.58–3.62 GHz) centered at 3.6 GHz, and 1470 MHz (4.93–6.4 GHz) centered at 5.5 GHz, which is useful for WiMAX and WLAN applications.

The far-field ($R \gg \frac{2D^2}{\lambda}$ (Friis equation)) radiation patterns and antenna gains are measured in an anechoic chamber. Measured radiation patterns at 3 GHz, 3.6 GHz, and 5.5 GHz are shown in Figs. 14(a)–(b), respectively. They exhibit the dipole pattern at elevation plane and omnidirectional pattern at azimuthal plane, which govern the significant directions for WiMAX and WLAN operating bands. The simulated and measured gain plots as a function of frequency are illustrated in Fig. 15. Measured peak gains 2.4 dBi, 3.07 dBi, and 4.64 dBi are inferred at 3 GHz, 3.6 GHz, and 5.5 GHz, respectively.

Table 2. Numerical results of simulated and experimental values of the proposed antenna.

Proposed antenna	Resonance frequency (GHz)	S_{11} (dB)	Impedance bandwidth (MHz)
Simulated	3.03	−19	80
	3.66	−24	50
	5.5	−19	1640
Measured	3	−12	40
	3.6	−16	40
	5.5	−17	1470

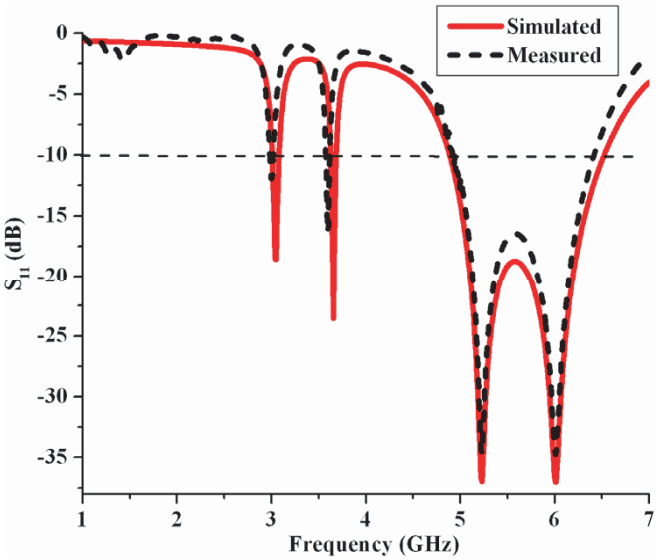

Figure 13. Simulated and experimental S_{11} (dB) characteristics.

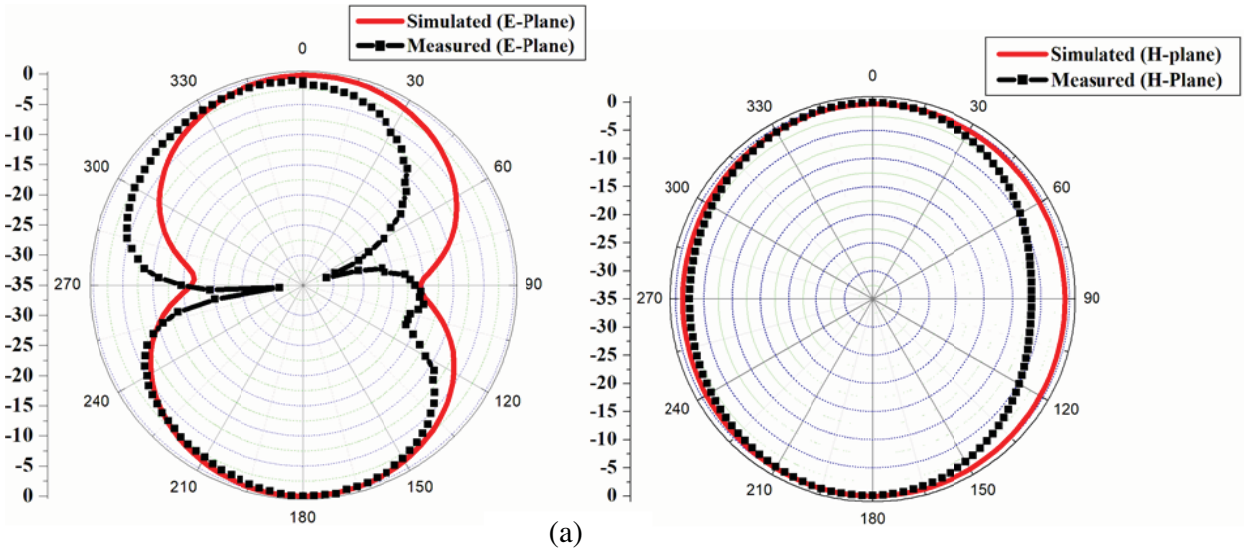

(a)

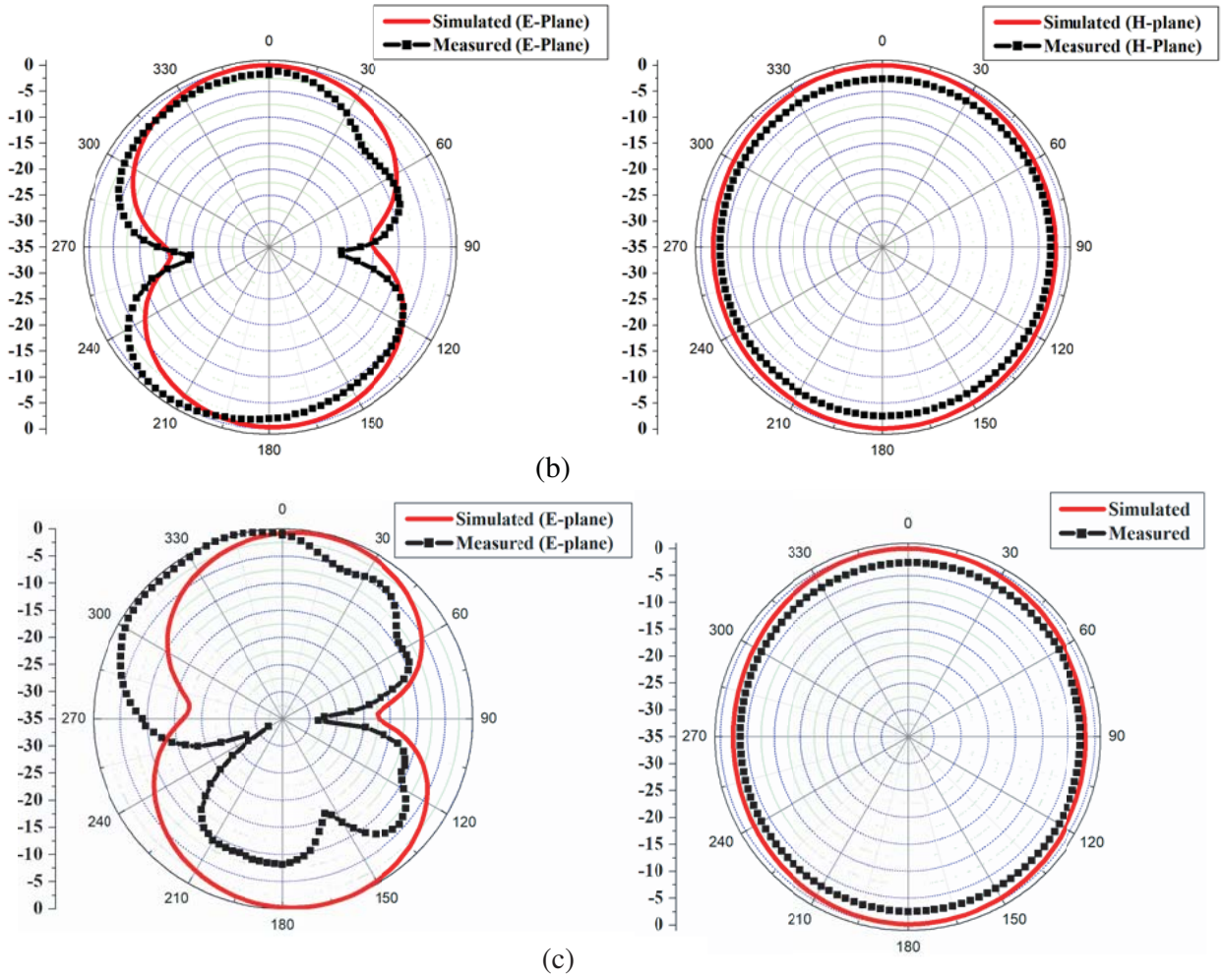

Figure 14. Simulated and measured far-field radiations (a) 3 GHz, (b) 3.6 GHz, and (c) 5.5 GHz.

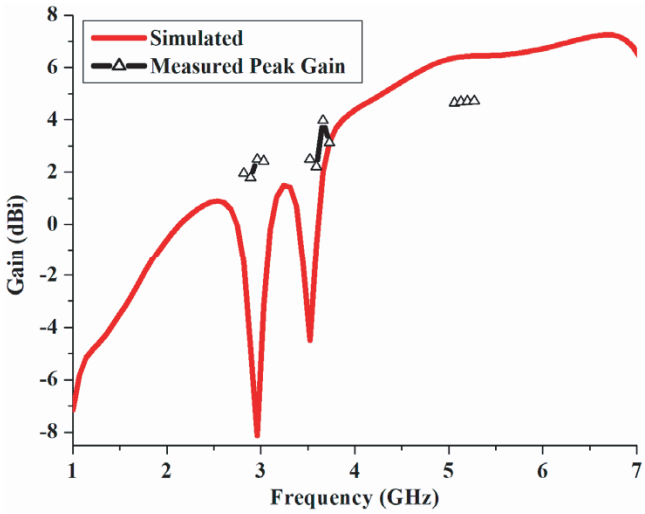

Figure 15. Gain plot of the proposed antenna.

6. CONCLUSION

A miniaturized CSRR based radiating element with offset-fed microstrip line is discussed for WiMAX and WLAN applications. The radiating element is reformed to arrange two pairs of complementary split rings, which also verifies negative permittivity presence, due to which new resonance frequencies are created. The parametric analysis of feed position, slit gap, and equivalent circuit of the proposed antenna has been studied for multiband abilities. The passband behaviour of the CSRR radiating element is explained by effective medium theory to validate the multiband characteristics. The measured input reflection coefficient, peak gain, and far-field patterns sufficient for the desired wireless applications.

REFERENCES

1. Daniel, R. S., R. Pandeeswari, and S. Raghavan, "A compact metamaterial loaded monopole antenna with offset-fed microstrip line for wireless applications," *AEU Int. J. Electron. Commun.*, Vol. 83, 88–94, 2018.
2. Caloz, C. and T. Itoh, *Electromagnetic Metamaterials: Transmission Line Theory and Microwave Applications*, John Wiley & Sons, Inc., New York, 2006.
3. Pandeeswari, R., "SRR and NBCSRR inspired CPW fed triple band antenna with modified ground plane," *Progress In Electromagnetics Research C*, Vol. 80, 111–118, 2018.
4. Xu, H.-X., G.-M. Wang, C.-X. Zhang, and Q. Peng, "Hilbert-shaped complementary single split ring resonator and low-pass filter with ultra-wide stopband, excellent selectivity and low insertion loss," *AEU Int. J. Electron. Commun.*, Vol. 65, No. 11, 901–905, 2011.
5. Karthikeyan, S. S. and R. S. Kshetrimayum, "Compact, harmonic suppressed power divider using open complementary split-ring resonator," *Microw. Opt. Technol. Lett.*, Vol. 53, No. 12, 2897–2899, 2011.
6. Phani Kumar, K. V. and S. S. Karthikeyan, "Wideband three section branch line coupler using triple open complementary split ring resonator and open stubs," *AEU Int. J. Electron. Commun.*, Vol. 69, No. 10, 1412–1416, 2015.
7. Daniel, R. S., R. Pandeeswari, and S. Raghavan, "Multiband monopole antenna loaded with complementary split ring resonator and C-shaped slots," *AEU Int. J. Electron. Commun.*, Vol. 75, 8–14, 2017.
8. Daniel, R. S., R. Pandeeswari, and S. Raghavan, "Design and analysis of open complementary split ring resonators loaded monopole antenna for multiband operation," *Progress In Electromagnetics Research C*, Vol. 78, 173–182, 2017.
9. Daniel, R. S., R. Pandeeswari, and S. Raghavan, "Offset-fed complementary split ring resonators loaded monopole antenna for multiband operations," *AEU Int. J. Electron. Commun.*, Vol. 78, 72–78, 2017.
10. Lu, M., J. Y. Chin, R. Liu, and T. J. Cui, "A microstrip phase shifter using complementary metamaterials," *International Conference on Microwave and Millimeter Wave Technology*, 1569–1571, 2008.
11. Rajabloo, H., V. A. Kooshki, and H. Oraizi, "Compact microstrip fractal Koch slot antenna with ELC coupling load for triple band application," *AEU Int. J. Electron. Commun.*, Vol. 73, 144–149, 2017.
12. Daniel, R. S., R. Pandeeswari, and S. Raghavan, "Dual-band monopole antenna loaded with ELC metamaterial resonator for WiMAX and WLAN applications," *Applied Physics A Materials Science & Processing*, Vol. 124, 570, 2018.
13. Bakır, M., M. Karaaslan, F. Karadağ, E. Ünal, O. Akgöl, F. Ö. Alkurt, and C. Sabah, "Metamaterial-based energy harvesting for GSM and satellite communication frequency bands," *Optical Engineering*, Vol. 57, No. 8, 087110, 2018.
14. Dincer, F., M. Karaaslan, S. Colak, E. Tetik, O. Akgol, O. Altıntas, and C. Sabah, "Multi-band polarization independent cylindrical metamaterial absorber and sensor application," *Modern Physics Letters B*, Vol. 30, No. 8, 1650095, 2016.

15. Altintas, O., E. Unal, O. Akgol, M. Karaaslan, F. Karadag, and C. Sabah, "Design of a wide band metasurface as a linear to circular polarization converter," *Modern Physics Letters B*, Vol. 31, No. 30, 1750274, 2017.
16. Daniel, R. S., R. Pandeeswari, and S. Raghavan, "Multiband monopole antenna loaded with complementary split ring resonator and C-shaped slots," *AEU Int. J. Electron. Commun.*, Vol. 75, 8–14, 2017.
17. Daniel, R. S., R. Pandeeswari, and S. Raghavan, "A miniaturized printed monopole antenna loaded with hexagonal complementary split ring resonators for multiband operations," *Int. J. RF Microw. Comput. Aided Eng.*, e21401, 2018.